



MiR-216b Promotes Osteoclastogenesis and Decreases Osteoclast Cholesterol Efflux by Targeting ABCG1*

YANG Wu-Zhou^{1)**}, LI Heng^{1)**}, YU Xiao-Hua^{2)**}, ZHANG Jie¹⁾, HUANG Xin-Yun¹⁾,
ZHAO Zhen-Wang¹⁾, CAO Qi^{1)***}, TANG Chao-Ke^{1)***}

¹⁾Institute of Cardiovascular Disease, Key Laboratory for Arteriosclerosis of Hunan Province, Hunan Province Cooperative Innovation Center for Molecular Target New Drug Study, the Second Affiliated Hospital, University of South China, Hengyang 421001, China;

²⁾Institute of Clinical Medicine, the Second Affiliated Hospital of Hainan Medical University, Haikou 460106, China)

Abstract Objective To investigate the function and the target gene of miR-216b in osteoclast differentiation and explore its effect on osteoclast cholesterol efflux. **Methods** The cell model of RAW264.7 osteoclast precursor cell differentiation induced by RANKL stimulation was established. Tartrate-resistant acid phosphatase (TRAP) staining assay was conducted to evaluate osteoclasts differentiation. MiR-216b target gene, ABCG1 3' untranslated region (3'UTR) sequence and free energy were predicted and analyzed by bioinformatics analyses and dual-luciferase reporter assays. MiR-216b mimic or inhibitor transfection was performed to verify the role of miR-216b in osteoclast differentiation. Liquid scintillation counting was used to measure [³H]-labeled cholesterol efflux from RAW264.7 macrophage-derived osteoclasts. The lipid accumulation in RAW264.7 macrophages was detected by high performance liquid chromatography (HPLC). Real-time quantitative PCR (RT-qPCR) and Western blot assays were used to assess the transcriptional and post-transcriptional levels of ABCG1 in osteoclasts. **Results** Our results showed that the number of osteoclasts, the average diameter of osteoclasts and the fusion index were significantly increased when cells were transfected with miR-216b mimic, as revealed by tartrate-resistant acid phosphatase-positive staining and microscopy assay. MiR-216b inhibitor showed the complete opposite outcome which brought additional evidence to our findings. Bioinformatics analysis and dual-luciferase reporter assays showed that miR-216b targets the 3'UTR of ABCG1. Moreover, miR-216b suppressed both the mRNA and protein levels of ABCG1 in osteoclasts. Besides, we found that silencing of ABCG1 by ABCG1 siRNA increased the number of osteoclasts, the average diameter of osteoclasts and the fusion index. MiR-216b reduced cholesterol efflux from osteoclasts by inhibiting ABCG1 expression. **Conclusion** Collectively, these findings suggest that miR-216b downregulates ABCG1 expression and inhibits osteoclast cholesterol efflux, which disturbs cholesterol homeostasis and promotes osteoclastogenesis.

Key words miR-216b, osteoclast, ABCG1, cholesterol efflux, osteoclastogenesis

DOI: 10.16476/j.pibb.2021.0014

Osteoporosis is widely considered as one of the major health problems in elderly people, especially menopausal women^[1-2]. This disease is featured by decreased bone mass and deteriorated bone microarchitecture, leading to bone fragility and an increased predisposition to fracture. Osteoclasts, a multinucleated cell type principally responsible for bone resorption, are differentiated from monocyte-macrophage precursors after induction of receptor activator of NF- κ B ligand (RANKL) and macrophage colony-stimulating factor (M-CSF)^[3]. Increased

osteoclast formation and activity have long been regarded as important contributors to bone loss and deterioration.

* This work was supported by a grant from The National Natural Science Foundation of China (81770461).

** These authors contributed equally to this work.

*** Corresponding author.

TANG Chao-Ke. Tel: 86-734-8281853, E-mail: tangchaoke@qq.com

CAO Qi. Tel: 86-734-8281853, E-mail: caoqi69@163.com

Received: April 14, 2021 Accepted: June 24, 2021

As an important part of cell membrane, cholesterol is closely related to cell metabolism. It is required for the fusion of pre-osteoclasts into multinucleated and mature osteoclasts. Also, cholesterol enhances the bone resorption by up-regulating the expression of tartrate-resistant acid phosphatase (TRAP). Accumulating evidence has revealed that the risk of developing osteoporosis is positively associated with cardiovascular disease and metabolic syndrome^[4-6]. Hypercholesterolemia is widely present in individuals with metabolic syndrome or cardiovascular disease. It has been reported that diet-induced hypercholesterolemia accelerates bone loss in mice, which is related to increased osteoclastic activity^[6-8]. Similarly, treatment of mouse peritoneal macrophages with cholesterol promotes osteoclast activity *via* upregulating interleukin-1 alpha (IL-1 α) expression^[9]. In contrast, it was found that high-density lipoprotein (HDL) or cyclodextrin facilitates cholesterol efflux from osteoclast precursor cells, which inhibits osteoclast activity driven by RANKL or M-CSF and promotes osteoclast apoptosis^[10]. Moreover, the expression of hydroxymethylglutaryl coenzyme-A (HMG-CoA) was found to be very low in osteoclasts and was not responsive to cyclodextrin treatment, suggesting an absence of feedback control of endogenous cholesterol biosynthesis in osteoclasts^[10-11]. This suggests the incapacity of osteoclasts to synthesize cholesterol and emphasizes the important role of cellular cholesterol homeostasis in osteoclast formation, survival and morphology.

ATP-binding cassette transporter G1 (ABCG1), a transmembrane half transporter, is widely expressed by macrophages and plays a pivotal role in promoting efflux of cholesterol and phosphatidylcholine onto HDL^[12-14]. Recently, several studies have shown that knockdown of ABCG1 in pre-osteoclasts leads to osteoclast fusion^[15-16]. Previous studies from our group also showed that HDL inhibits osteoclastogenesis through upregulation of ABCG1 expression^[17]. Thus, a better understanding of the relationship between ABCG1 and its regulators is essential to develop new strategies for the prevention and treatment of osteoporosis.

MicroRNAs (miRNAs) are small, endogenous, and evolutionarily conserved noncoding RNAs with approximately 22 nucleotides in length and play

crucial roles in posttranscriptional regulation of gene expression^[18-19]. Numerous studies have shown that many miRNAs have been identified to involve in osteoclastogenesis^[20-21]. MiR-216b, a highly conserved miRNA among different species, is implicated in tumor progression^[22-24]. Recent studies have found that miR-216a can promote osteoblast differentiation by regulating the c-Cbl-mediated PI3K/AKT pathway^[25]. However, the role of miR-216b in osteoclasts is still poorly understood.

In the present study, we investigated the mechanism underlying miR-216b promotion of osteoclastogenesis and suppression of cholesterol efflux and the roles of ABCG1 in osteoclast.

1 Materials and methods

1.1 Cell culture and treatment

The human embryonic kidney cell line 293T and mouse macrophage cell line RAW264.7 were purchased from Cell Bank, Chinese Academy of Sciences (Shanghai, China). Both RAW264.7 and 293T cells were cultured in Dulbecco's Modified Eagle Medium (DMEM) containing 10% fetal bovine serum (FBS, Gibco BRL, USA) with 5% CO₂ at 37° C. RAW264.7 cells were seeded into 24-well plates (4×10⁴ cells/well) and incubated with 50 pg/L M-CSF (ab259396, Abcam, Cambridge, USA) and 50 pg/L RANKL (ab129136, Abcam, Cambridge, USA) for 4 d to induce osteoclast differentiation.

1.2 Tartrate-resistant acid phosphatase (TRAP) staining assay

Differentiated cells were assessed by TRAP staining as previously described^[17]. Briefly, RANKL and M-CSF-induced RAW264.7 cells were fixed in 4% paraformaldehyde at room temperature for 30 min. Thereafter, cells were stained for TRAP using a leukocyte acid phosphatase assay kit (Sigma, St Louis, USA) according to the manufacturer's protocol. After removal of the TRAP solution, the plate was washed three times with phosphate-buffered saline (PBS). The stained cells were observed and counted using an inverted microscope. TRAP-positive cells with more than or equal to 3 nuclei were regarded as osteoclasts.

1.3 Cell transfection

MiR-216b inhibitors, miR-216b mimics, and miR-216b negative control (NC) were obtained from

Ribobio (Guangzhou, China). The ABCG1 target sequence selected for siRNA synthesis was as follows: 5'-TCGTATCTTATCTGTAGAGAA-3'. RAW264.7 cells were seeded into 6-well plates and transfected with ABCG1 siRNA, miR-216b mimics, miR-216b inhibitors and miR-216b NC using Lipofectamine 2000 (Invitrogen, Shanghai, China) following the manufacturer's protocol. The transfected cells were collected at 24 h for further experimental analyses.

1.4 Luciferase reporter assay

The cDNA fragment corresponding to the entire ABCG1 3'UTR was amplified by RT-qPCR from total RNA extracted from RAW264.7 cells. The 3'UTR sequences of ABCG1 containing the mutant or wild-type binding sites were cloned into the pmirGLO dual-luciferase vector (Promega, Madison, WI, USA). 293T cells (1×10^6 cells/well) were seeded into 12-well plates for 24 h. Cells were then co-transfected using Lipofectamine 2000 with miR-216b mimic, mutant (Mut) or wild-type (WT) ABCG1 3'UTR. After 48 h, cells were harvested and lysed and the luciferase activity of cells was then measured using a dual-luciferase assay kit (Promega, Madison, WI, USA). Renilla luciferase activity of each group was normalized to that of corresponding firefly luciferase activity.

1.5 Western blot

Cells were lysed for protein extraction using radioimmunoprecipitation assay (RIPA) buffer (Solarbio Life Sciences, Beijing, China) and protein concentrations were examined using a BCA assay kit (CW BIO, Beijing, China), as previously described^[26]. Proteins (20 μ g per lane) were separated by 6% SDS polyacrylamide gel electrophoresis (SDS-PAGE) and then transferred to polyvinylidene fluoride (PVDF) membranes. The membranes were blocked with 5% fat-free dry milk-TBST buffer (Tris-buffered saline containing 0.1% Tween-20) at room temperature for 4 h and then immunoblotted with respective primary antibodies overnight at 4°C. Then, the membranes were rinsed with TBST three times (10 min each time) and subsequently incubated with a horseradish peroxidase-conjugated goat anti-rabbit secondary antibody at a dilution of 1 : 5 000 for 2 h at room temperature. Finally, the protein bands were detected by the enhanced chemiluminescence reaction and then quantified with a gel imaging system (Tanon,

Shanghai, China).

1.6 Real-time quantitative polymerase chain reaction (RT-qPCR)

Total RNAs from RAW264.7 cells were extracted using TRIzol reagent (Invitrogen, Shanghai, China) following the reagent manufacturer's protocol. 2 μ g of cDNA fragments was obtained by reverse transcription from RNA using the TaqMan™ reverse transcription reagent kit (Applied Biosystems, Foster City, USA). Relative quantitative real-time PCR was carried out by SYBR Green chemistry using a Light Cycler Run 5.32 Real-Time PCR System (Roche, Beijing, China). Sequences of quantitative real-time PCR primers are as follows: ABCG1 sense 5'-GGTGGTCTCGCTGATGAAAG-3' and anti-sense 5'-CTGCTGGGTTGTGGTAGGTT-3'; β -actin sense 5'-ATCGTGCGTGACATT AAGGAGAAG-3' and anti-sense 5'-AGGAAGGAAGGCTGGAAG AGTG-3'. All real-time PCR products were evaluated by melt curve analyses. Quantitative measurements used in this study were evaluated using the $\Delta\Delta C_t$ method and β -actin was used as the internal control gene.

1.7 Cellular cholesterol efflux assay

RAW264.7 cells were cultured and differentiated as indicated above, and radiolabeled with 5 mCi/L of [³H]-cholesterol (Sigma, St Louis, USA) for 24 h in media containing 0.2% bovine serum albumin (BSA). Afterward, cells were washed with fresh media and then treated conditionally as indicated. Then, the cells were rinsed again with PBS and cultured in media supplemented with HDL (50 ng/L) for 24 h. [³H]-cholesterol present in medium was quantified by liquid scintillation counting. Finally, the percent cholesterol effluxed from cells was evaluated by the equation: (total media counts / (total cellular counts + total media counts)) \times 100%.

1.8 High-performance liquid chromatography (HPLC) assay

To detect lipid levels in RAW264.7 cells, the HPLC analysis was performed in accordance with the method described previously^[27-28]. In brief, after RAW264.7 cells were transformed into osteoclast by incubating with RANKL and M-CSF, miR-216b inhibitors, miR-216b mimics or miR-216b NC were added and incubated for 24 h. Then, transfected cells were detached by trypsin/EDTA. The sterol analyses were carried out using the HPLC system (Model 2790, controlled with Empower Pro software, Waters

Corporation, Milford, MA). Sterols were measured using a photodiode array detector (model 996, Waters Corporation, Milford, MA). Analysis of sterol was conducted after elution with acetonitrile-isopropanol 30 : 70 (v/v). Absorbance at 210 nm was examined and data were analyzed by TotalChrom software from PerkinElmer (Shanghai, China).

1.9 Nuclear pyknosis assessment

RAW264.7 cells were treated with M-CSF and RANKL, followed by treatment of miR-216b inhibitors, miR-216b mimics, or miR-216b NC. Osteoclast differentiation was assessed by TRAP staining after 3–4 days of incubation. TRAP-positive multinucleated osteoclast nuclear pyknosis was examined under the microscope.

1.10 Statistical analysis

Data are represented as the means \pm SD of at least three independent experiments. Mean values were compared by one-way analysis of variance through Graphpad Prism 6 software. Statistical analysis was done using statistical software SPSS 18.0 (SPSS Inc., Chicago, IL, USA). Statistical differences were considered significant when $P < 0.05$.

2 Results

2.1 MiR-216b is up-regulated in osteoclastogenesis induced by M-CSF and RANKL

We used RT-qPCR to detect miR-216b expression during osteoclastogenesis. MiR-216b was markedly increased in RAW264.7 osteoclast precursor cells in 2 and 4 d following the induction of M-CSF and RANKL (Figure 1a). On the 4th day after stimulation of M-CSF and RANKL, miR-216b expression was markedly upregulated during primary osteoclast differentiation (Figure 1b).

2.2 MiR-216b promotes osteoclast formation

To explore the roles of miR-216b in osteoclast formation, we used RAW264.7 cells as osteoclast precursor cells and treated them with 50 pg/L M-CSF and 50 pg/L RANKL for differentiation and fusion. We cultured the cells with miR-216b mimics at distinct concentrations (10, 20, 40, 80 nmol/L) for 48 h or 80 nmol/L miR-216b mimics for various time courses (0, 12, 24, 48 h). Then, osteoclast differentiation was detected by TRAP staining. Our results showed that treatment with miR-216b mimics increased the number of TRAP-positive osteoclasts

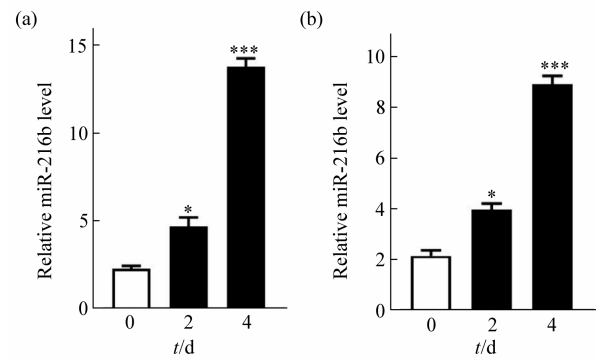


Fig. 1 The miR-216 expression during osteoclastogenesis

The expression of miR-216b was increased during osteoclast differentiation in both RAW264.7 cells (a) and primary osteoclast (b). * $P < 0.05$ vs. 0 d, *** $P < 0.001$ vs. 0 d.

(Figure 2a, g), the average diameter of osteoclasts (Figure 2b, h), and the fusion index (Figure 2c, i) in time- and concentration-dependent manners. Afterward, we treated RAW264.7 cells with various concentrations of miR-216b inhibitor (10, 20, 40, 80 nmol/L) for 48 h or with 40 nmol/L miR-216b inhibitors for different times (0, 12, 24, 48 h). In contrast, RAW264.7 cells transfected with miR-216b inhibitors showed the opposite effect (Figure 2d–i). The fusion index and the average diameter are important indicators for osteoclast formation. Besides, treatment with miR-216b inhibitors markedly upregulated the ratio of osteoclasts with nuclear pyknosis (Figure 2j), suggesting that miR-216b inhibitor promotes osteoclast apoptosis. Taken together, these data suggest that miR-216 facilitates osteoclast precursor fusion and osteoclast formation.

2.3 MiR-216b is highly conserved among mammals and is predicted to bind to ABCG1 3'UTR

Target gene prediction programs showed that the 3'UTR of ABCG1 transcripts in most animal species contain the putative binding sites for miR-216b (Figure 3a). The binding site is highly conserved across various mammalian species, indicating that miR-216b is functionally important for the evolution of species (Figure 3b). RNAhybrid data showed that the free energy scores for the hybridization between miR-216b and ABCG1 3'UTR are very low in mice (Figure 3c). These data indicate that ABCG1 may be a putative target of miR-216b.

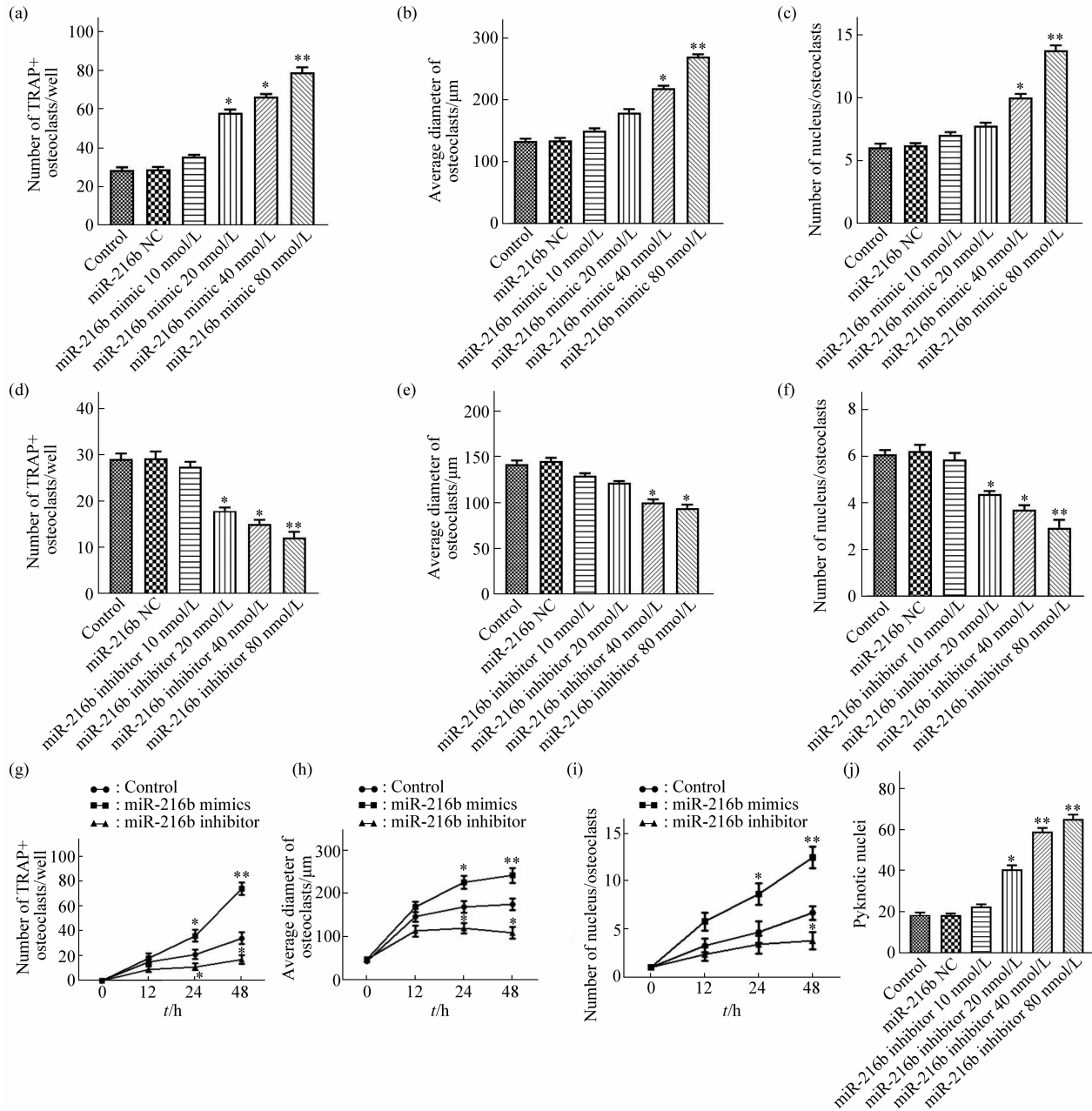


Fig. 2 MiR-216b promotes osteoclast formation

(a-i) RAW264.7 cells were cultured as osteoclast precursors and treated with M-CSF (50 pg/L) and RANKL (50 pg/L) for the differentiation and fusion. The cells were transfected with miR-216b mimics or miR-216b inhibitors at different concentrations (10, 20, 40, 80 nmol/L) for 48 h or with 80nmol/L of them for different periods of time (0, 12, 24, 48 h). (a, d, g) The numbers of TRAP-positive multinucleated cells were detected under a microscope. Cells with 3 or more than 3 nuclei were counted as osteoclasts. (b, e, h) TRAP-positive staining assay was conducted on days 3 and 4 after treatment. 40 osteoclasts were randomly selected for the measurement of the average diameter. (c, f, i) Fusion index, calculated as the ratio of total numbers of nucleus to total multinucleated osteoclast numbers. (j) Pyknotic nuclei were observed by the microscope. All results were presented as $\bar{x} \pm s$ from three independent experiments. * $P < 0.05$ vs. control or miR-216b NC, ** $P < 0.01$ vs. control or miR-216b NC.

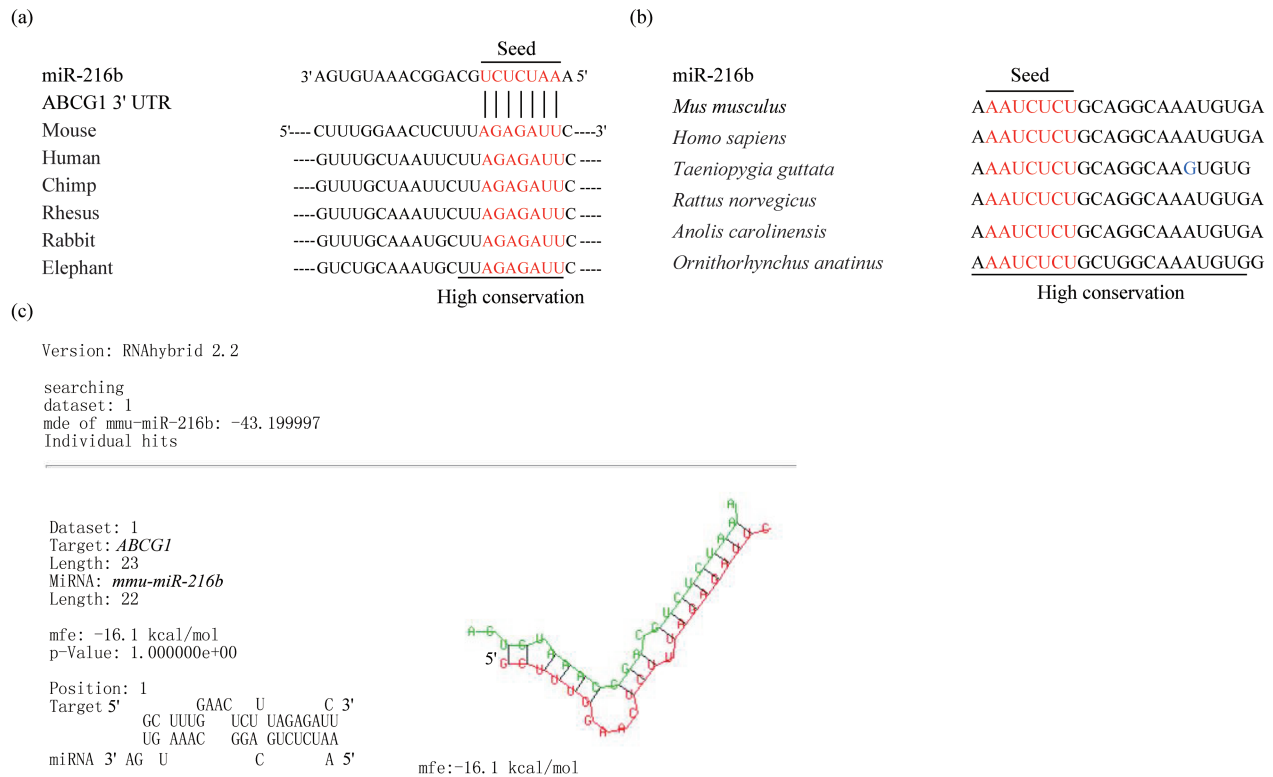


Fig. 3 Prediction of the miR-216b target site in the ABCG1 3'UTR

(a) miR-216b has the same bases and is highly conserved among various species (miRDB). (b) Sequence alignment of the miR-216b mature sequence binding to the 3'UTR of ABCG1 in multiple species. (c) The free energy scores (in RNAhybrid) for miR-216b-ABCG1 3'UTR hybridization in mice.

2.4 MiR-216b directly targets ABCG1 3'UTR and inhibits ABCG1 expression

To identify if ABCG1 is a direct target of miR-216b, we carried out a dual-luciferase reporter assay in 293T cells. The luciferase reporter assay revealed that the promoter activity of wild-type ABCG1 3'UTR but not mutant ABCG1 3'UTR in the 293T cells transfected with miR-216b mimics was significantly diminished (Figure 4a). These observations indicate that miR-216b regulates ABCG1 expression by directly targeting the 3'UTR of ABCG1.

Next, we determined the effect of miR-216b on ABCG1 expression in M-CSF and RANKL-induced RAW264.7 cells. The cells were treated with distinct concentrations of miR-216b mimics (10, 20, 40, 80 nmol/L) for 48 h or with 80 nmol/L miR-216b mimics for various durations (0, 12, 24, 48 h). The protein and mRNA levels of ABCG1 were detected using Western blot and qPCR analyses, respectively. As shown in Figure 4b, c, treatment of RAW264.7 macrophage-derived osteoclasts with miR-216b

mimics significantly decreased the protein levels of ABCG1 in time- and concentration-dependent manners. Although the levels of osteoclast ABCG1 mRNA (Figure 4d) have a decreasing trend when transfected with 0–40 nmol/L miR-216b mimics, it is not statistically significant compared with those of the control group. Only when the concentration of miR-216b mimics was 80 nmol/L (Figure 4d) or transfected with miR-216b mimics for 48 h (Figure 4e), ABCG1 mRNA levels were significantly reduced. This indicates that miR-216b could affect both mRNA degradation and protein translation, but mainly inhibits protein translation. By contrast, RAW264.7 cells treated with miR-216b inhibitors displayed the opposite effect (Figure 4f–i). As shown in Figure 4f, ABCG1 protein level increased most significantly when the concentration of transfected miR-216b inhibitors was 40 nmol/L. Also, ABCG1 mRNA levels were markedly elevated only in the cells treated with 40 nmol/L miR-216b inhibitors for 48 h (Figure 4h, i). It is possible that high concentrations of miR-216b

inhibitors accelerate cell apoptosis, which in turn increases ABCG1 mRNA degradation. Collectively,

these data suggest that ABCG1 is a target gene of miR-216b during osteoclast differentiation.

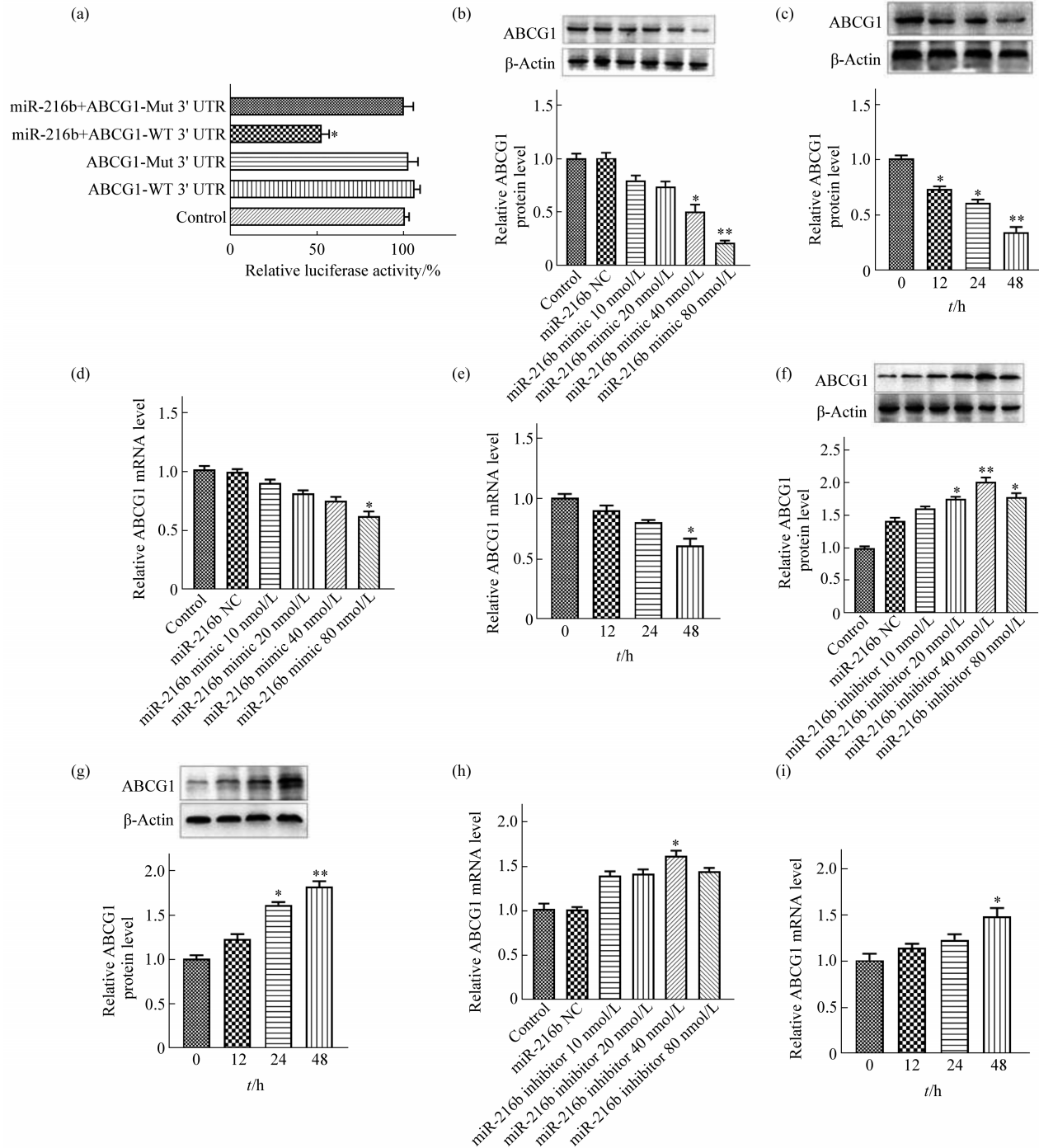


Fig. 4 MiR-216b inhibits ABCG1 expression by directly targeting ABCG1

(a) Luciferase activity was assessed using luciferase reporter assay in 293T cells transfected with a luciferase reporter plasmid containing mutant (Mut) or wild-type (WT) ABCG1 3'UTR and miR-216b mimic. (b-i) RAW264.7 macrophage-derived osteoclasts were transfected with miR-216b mimics and miR-216b inhibitors at different concentrations (10, 20, 40, 80 nmol/L) for 48 h or with 80 nmol/L of them for different periods of time (0, 12, 24, 48 h) to examine the effects of miR-216b on ABCG1 expression. The mRNA and protein levels of ABCG1 in RAW264.7 cells were determined by RT-qPCR and Western blot analyses, respectively. All results are expressed as $\bar{x} \pm s$ from three independent experiments. * $P < 0.05$ vs. control or miR-216b NC, ** $P < 0.01$ vs. control or miR-216b NC.

2.5 MiR-216b promotes osteoclast formation and reduces cholesterol efflux by suppressing ABCG1 expression

We further determined whether miR-216b promotes osteoclastogenesis by inhibiting ABCG1 expression. M-CSF and RANKL-treated RAW264.7 cells were transfected with miR-216b inhibitors, miR-216b mimics, or co-transfected with miR-216b inhibitors and ABCG1 siRNA. The protein and mRNA expression levels of ABCG1 were assessed by Western blot and qPCR analyses, respectively.

Osteoclast formation was measured by TRAP staining. As shown in Figure 5a–c, treatment with miR-216b inhibitors and ABCG1 siRNA significantly increased the number of multinucleated osteoclasts, the average diameter of osteoclasts and the fusion index compared with the miR-216b inhibitor-treated group. Moreover, the protein (Figure 5d) and mRNA (Figure 5e) levels of ABCG1 were markedly increased by miR-216b inhibitors and decreased by silencing ABCG1. These results suggest that ABCG1 is involved in miR-216b-induced osteoclast formation.

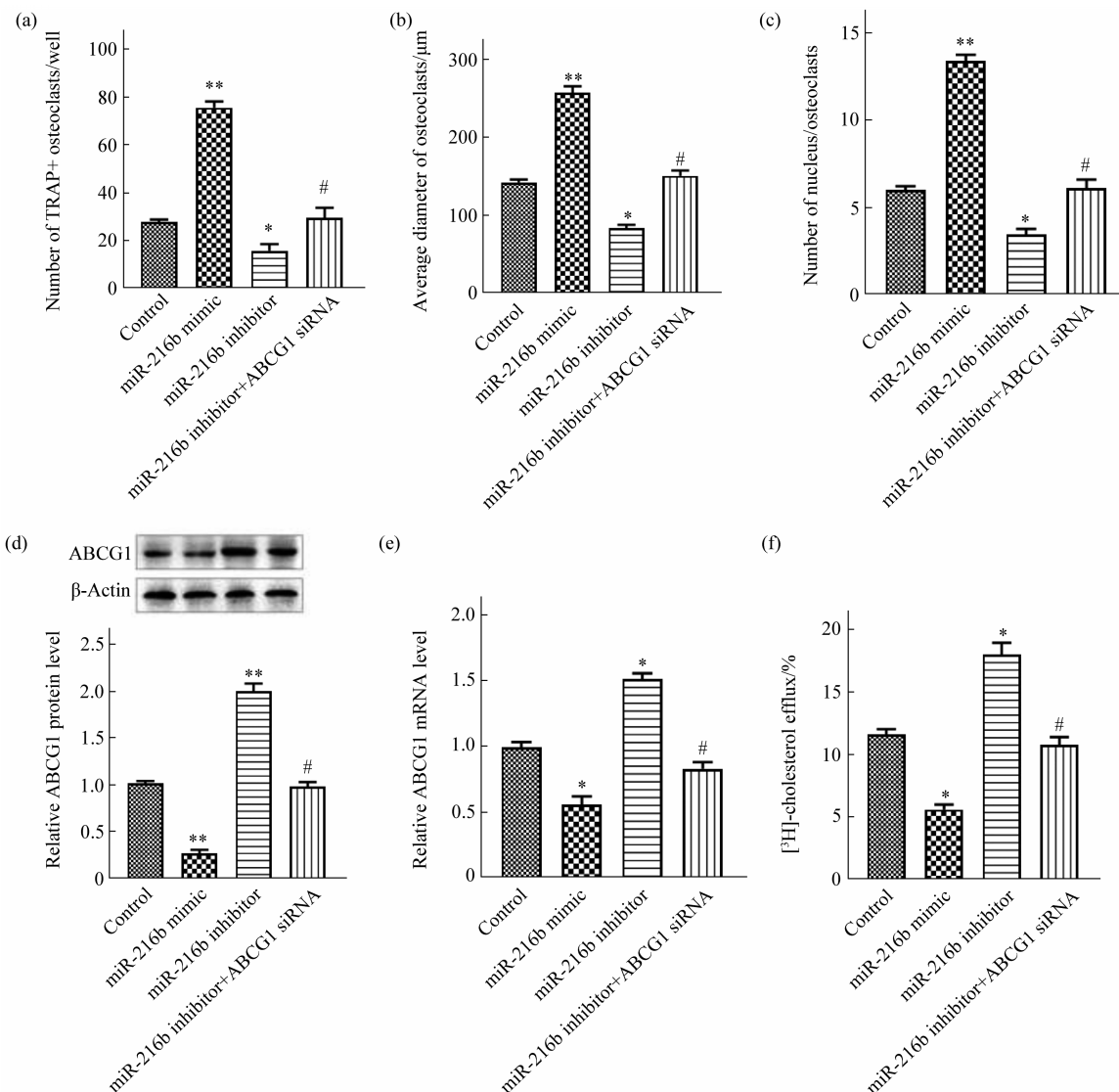


Fig. 5 MiR-216b promotes osteoclast formation and suppresses cholesterol efflux by downregulating ABCG1

(a–f) RAW264.7 macrophage-derived osteoclasts were treated with miR-216b mimics, miR-216b inhibitors or co-treated with miR-216b inhibitors and ABCG1 siRNA. (a, b) The protein and mRNA levels of ABCG1 were determined by Western blot and RT-qPCR analyses, respectively. (c–e) Osteoclast formation was assessed by TRAP staining. (f) Cholesterol efflux was measured by liquid scintillation counter. All results are expressed as $\bar{x} \pm s$ from three independent experiments. * $P < 0.05$ vs. control, ** $P < 0.01$ vs. control. # $P < 0.05$ vs. miR-216b inhibitor.

Cholesterol plays a crucial role in osteoclast differentiation. ABCG1 is essential for the maintenance of cellular cholesterol homeostasis. Thus, we performed a cholesterol efflux assay to examine whether miR-216b's promotion of osteoclast cholesterol efflux is dependent on ABCG1. As shown in Figure 5f, the rate of osteoclast cholesterol efflux was strikingly decreased in the miR-216b mimic-treated group but increased in the miR-216b inhibitor-treated group compared with the control group. Moreover, co-transfected with miR-216b inhibitors

and ABCG1 siRNA markedly reduced osteoclast cholesterol efflux compared with the miR-216b inhibitor-treated group. Besides, total lipid amounts in RAW264.7 cells were detected by HPLC. As shown in Table 1, free cholesterol (FC), total cholesterol (TC), and cholesteryl ester (CE) contents were greatly increased by miR-216b mimics. The decreased total lipid amounts by miR-216b inhibitors were restored after silencing of ABCG1. These results suggest that miR-216b reduces cholesterol efflux from osteoclasts by inhibiting ABCG1 expression.

Table 1 Effects of miR-216b on the lipid levels in RAW264.7 macrophages

	TC/(mg·g ⁻¹)	FC/(mg·g ⁻¹)	CE/(mg·g ⁻¹)	(CE/TC)%
Control	462.5±21.8	173.9±14.9	288.6±14.9	62.4
miR-216b mimic	569.7±27.5*	205.6±13.5*	364.1±16.8*	63.9
miR-216b inhibitor	342.7±25.3*	132.4±19.6*	210.3±12.4*	61.3
miR-216b inhibitor + ABCG1 siRNA	473.6±26.3 [#]	177.5±21.7 [#]	296.1±15.7 [#]	62.5

TC, total cholesterol; FC, free cholesterol; CE, cholesterol ester. Lipid levels were determined by HPLC. The data were the $\bar{x} \pm s$ from three independent experiments. * $P < 0.05$ vs. control group. [#] $P < 0.05$ vs. inhibitor group.

3 Discussion

Numerous studies have shown that dyslipidemia is a key risk factor for osteoporosis^[29-30]. Lipid metabolic disorder, especially hypercholesterolemia, can affect bone cells systemically and locally, resulting in the development of pathological bone conditions^[31]. However, the molecular mechanisms that underline the link between cholesterol metabolism and bone formation are still incompletely understood. In the present study, we explored the effects of miR-216b on osteoclast formation and the underlying molecular mechanisms. Our findings showed that miR-216b decreases the efflux of cholesterol from osteoclasts by inhibiting ABCG1 expression, leading to lipid raft dysfunction and subsequent osteoclast formation and survival.

A large number of miRNAs have crucial roles in regulating osteoclast differentiation. For instance, miR-125a-5p positively modulates RANKL-induced osteoclastogenesis by targeting TNF receptor superfamily member 1B gene (TNFRSF1B)^[32]. It has been found that miR-199a-5p promotes RANKL-mediated osteoclast differentiation by inhibiting Mafk^[33]. MiR-27a decreases adipogenesis and facilitates osteogenesis *via* repression of peroxisome proliferator-activated receptor (PPAR γ) and

gremlin 1^[34]. Besides, miR-503 was found to suppress osteoclast differentiation by inhibiting RANK expression^[35]. Although there are increasing studies on miRNAs involved in the modulation of bone remodeling, the precise role of miR-216b in osteoclast formation still needs further investigation. Here, we observed that treatment of miR-216b mimics markedly increased the number of TRAP-positive osteoclasts. In addition, the average diameter of osteoclasts and the fusion index were strikingly increased in RAW264.7 osteoclast precursor cells in response to miR-216b overexpression, which was consistent with an increase of TRAP staining activity in cells, further verified the promotive effect exerted by miR-216b on osteoclast differentiation.

MiRNAs have been reported to negatively modulate gene expression by base-pairing with complementary sequences in the 3'UTR of target mRNAs and targeting them for mRNA degradation or translational suppression of protein synthesis^[36], which supported our findings that miR-216b exerted an inhibitor effect on the expression of ABCG1 by binding to the 3'UTR of ABCG1. Previous studies from our group and others have found that ABCG1 overexpression protects against atherosclerosis by reducing lipid accumulation in macrophage^[37-38]. Recently, ABCG1 has also been identified as a key

factor affecting osteoclast formation due to its ability to mediate the efflux of cholesterol and phosphatidylcholine to HDL^[15-17]. Our findings showed that silencing of ABCG1 increased the number of TRAP-positive osteoclasts, the average diameter of osteoclasts and the fusion index, suggesting that ABCG1 knockdown promotes osteoclast differentiation. In addition, our study revealed that miR-216b impairs cholesterol efflux from osteoclasts by inhibiting ABCG1 expression. Taken together, we conclude that miR-216b inhibits cholesterol efflux from osteoclasts and promotes osteoclast differentiation, which is likely to be mediated by repression of ABCG1 expression. Thus, our study demonstrates that miR-216b inhibits cholesterol efflux from osteoclasts and promotes osteoclast differentiation, which is likely to be mediated by repression of ABCG1 expression. However, there have been several limitations to be considered. We did not conduct animal model experiments to detect the *in vivo* effects of miR-216b on ABCG1 expression and bone formation. Besides, we did not examine the effect of miR-216b on osteoclast apoptosis. The future studies should be designed to address these limitations.

4 Conclusion

The present study demonstrated that miR-216b promotes osteoclast differentiation and decreases osteoclast cholesterol efflux by targeting ABCG1. This provides direct evidence for the association between miR-216b and ABCG1 and the critical roles of them in osteoclast formation and cholesterol metabolism. With continued efforts, delivery of miR-216b antagonist or prevention of endogenous miR-216b expression may be a promising approach to prevent and treat osteoporosis.

References

- [1] Black D M, Rosen C J. Clinical practice. Postmenopausal osteoporosis. *N Engl J Med*, 2016, **374**(3): 254-262
- [2] Zaw J J T, Howe P R C, Wong R H X. Postmenopausal health interventions: time to move on from the women's health initiative?. *Ageing Res Rev*, 2018, **48**: 79-86
- [3] Boyce B F. Advances in the regulation of osteoclasts and osteoclast functions. *J Dent Res*, 2013, **92**(10): 860-867
- [4] Covic A, Vervloet M, Massy Z A, *et al.* Bone and mineral disorders in chronic kidney disease: implications for cardiovascular health and ageing in the general population. *Lancet Diabetes Endocrinol*, 2018, **6**(4): 319-331
- [5] Halade G V, Rahman M M, Williams P J, *et al.* High fat diet-induced animal model of age-associated obesity and osteoporosis. *J Nutr Biochem*, 2010, **21**(12): 1162-1169
- [6] Pelton K, Krieder J, Joiner D, *et al.* Hypercholesterolemia promotes an osteoporotic phenotype. *Am J Pathol*, 2012, **181**(3): 928-936
- [7] Tarakida A, Iino K, Abe K, *et al.* Hypercholesterolemia accelerates bone loss in postmenopausal women. *Climacteric*, 2011, **14**(1): 105-111
- [8] Mandal C C. High cholesterol deteriorates bone health: new insights into molecular mechanisms. *Front Endocrinol*, 2015, **6**: 165
- [9] Sjogren U, Mukohyama H, Roth C, *et al.* Bone-resorbing activity from cholesterol-exposed macrophages due to enhanced expression of interleukin-1alpha. *J Dent Res*, 2002, **81**(1): 11-16
- [10] Luegmayr E, Glantschnig H, Wesolowski G A, *et al.* Osteoclast formation, survival and morphology are highly dependent on exogenous cholesterol/lipoproteins. *Cell Death Differ*, 2004, **11**: S108-S118
- [11] Bergstrom J D, Bostedor R G, Masarachia P J, *et al.* Alendronate is a specific, nanomolar inhibitor of farnesyl diphosphate synthase. *Arch Biochem Biophys*, 2000, **373**(1): 231-241
- [12] Tarling E J, Edwards P A. ATP binding cassette transporter G1 (ABCG1) is an intracellular sterol transporter. *Proc Natl Acad Sci USA*, 2011, **108**(49): 19719-19724
- [13] Tang S L, Chen W J, Yin K, *et al.* PAPP-A negatively regulates ABCA1, ABCG1 and SR-B1 expression by inhibiting LXRalpha through the IGF-I-mediated signaling pathway. *Atherosclerosis*, 2012, **222**(2): 344-354
- [14] Kobayashi A, Takanezawa Y, Hirata T, *et al.* Efflux of sphingomyelin, cholesterol, and phosphatidylcholine by ABCG1. *J Lipid Res*, 2006, **47**(8): 1791-1802
- [15] Irie A, Yamamoto K, Miki Y, *et al.* Phosphatidylethanolamine dynamics are required for osteoclast fusion. *Sci Rep*, 2017, **7**: 46715
- [16] Kitano V J F, Ohyama Y, Hayashida C, *et al.* LDL uptake-dependent phosphatidylethanolamine translocation to the cell surface promotes fusion of osteoclast-like cells. *J Cell Sci*, 2020, **133**(10): jcs243840
- [17] Huang X, Lv Y, He P, *et al.* HDL impairs osteoclastogenesis and induces osteoclast apoptosis *via* upregulation of ABCG1 expression. *Acta Biochim Biophys Sin*, 2018, **50**(9): 853-861
- [18] Iwakawa H O, Tomari Y. The functions of microRNAs: mRNA decay and translational repression. *Trends Cell Biol*, 2015, **25**(11): 651-665
- [19] Huntzinger E, Izaurralde E. Gene silencing by microRNAs: contributions of translational repression and mRNA decay. *Nat Rev Genet*, 2011, **12**(2): 99-110
- [20] Van Wijnen A J, Van De Peppel J, Van Leeuwen J P, *et al.* MicroRNA functions in osteogenesis and dysfunctions in osteoporosis. *Curr Osteoporos Rep*, 2013, **11**(2): 72-82

- [21] Tang P, Xiong Q, Ge W, *et al.* The role of microRNAs in osteoclasts and osteoporosis. *RNA Biol*, 2014, **11**(11): 1355-1363
- [22] Shan Y, Ma J, Pan Y, *et al.* LncRNA SNHG7 sponges miR-216b to promote proliferation and liver metastasis of colorectal cancer through upregulating GALNT1. *Cell Death Dis*, 2018, **9**(7): 722
- [23] Ferino A, Miglietta G, Picco R, *et al.* MicroRNA therapeutics: design of single-stranded miR-216b mimics to target KRAS in pancreatic cancer cells. *RNA Biol*, 2018, **15**(10): 1273-1285
- [24] Liu Y, Niu Z, Lin X, *et al.* MiR-216b increases cisplatin sensitivity in ovarian cancer cells by targeting PARP1. *Cancer Gene Ther*, 2017, **24**(5): 208-214
- [25] Li H, Li T, Fan J, *et al.* MiR-216a rescues dexamethasone suppression of osteogenesis, promotes osteoblast differentiation and enhances bone formation, by regulating c-Cbl-mediated PI3K/AKT pathway. *Cell Death Differ*, 2015, **22**(12): 1935-1945
- [26] Tang X E, Li H, Chen L Y, *et al.* IL-8 negatively regulates ABCA1 expression and cholesterol efflux *via* upregulating miR-183 in THP-1 macrophage-derived foam cells. *Cytokine*, 2019, **122**: 154385
- [27] He P P, Ouyang X P, Tang Y Y, *et al.* MicroRNA-590 attenuates lipid accumulation and pro-inflammatory cytokine secretion by targeting lipoprotein lipase gene in human THP-1 macrophages. *Biochimie*, 2014, **106**: 81-90
- [28] Lu Q, Tang S L, Liu X Y, *et al.* Tertiary-butylhydroquinone upregulates expression of ATP-binding cassette transporter A1 *via* nuclear factor E2-related factor 2/heme oxygenase-1 signaling in THP-1 macrophage-derived foam cells. *Circ J*, 2013, **77**(9): 2399-2408
- [29] Tintut Y, Demer L L. Effects of bioactive lipids and lipoproteins on bone. *Trends Endocrinol Metab*, 2014, **25**(2): 53-59
- [30] Lin X, Peng C, Greenbaum J, *et al.* Identifying potentially common genes between dyslipidemia and osteoporosis using novel analytical approaches. *Mol Genet Genomics*, 2018, **293**(3): 711-723
- [31] Papachristou D J, Blair H C. Bone and high-density lipoprotein: the beginning of a beautiful friendship. *World J Orthop*, 2016, **7**(2): 74-77
- [32] Sun L, Lian J X, Meng S. MiR-125a-5p promotes osteoclastogenesis by targeting TNFRSF1B. *Cell Mol Biol Lett*, 2019, **24**: 23
- [33] Guo K, Zhang D, Wu H, *et al.* MiRNA-199a-5p positively regulated RANKL-induced osteoclast differentiation by target Mafk protein. *J Cell Biochem*, 2018, **120**(5): 7024-7031
- [34] Gu C, Xu Y, Zhang S, *et al.* MiR-27a attenuates adipogenesis and promotes osteogenesis in steroid-induced rat BMSCs by targeting PPARgamma and GREM1. *Sci Rep*, 2016, **6**: 38491
- [35] Chen C, Cheng P, Xie H, *et al.* MiR-503 regulates osteoclastogenesis *via* targeting RANK. *J Bone Miner Res*, 2014, **29**(2): 338-347
- [36] Bartel D P. MicroRNAs: target recognition and regulatory functions. *Cell*, 2009, **136**(2): 215-233
- [37] Out R, Hoekstra M, Meurs I, *et al.* Total body ABCG1 expression protects against early atherosclerotic lesion development in mice. *Arterioscler Thromb Vasc Biol*, 2007, **27**(3): 594-599
- [38] Zhao Z W, Zhang M, Chen L Y, *et al.* Heat shock protein 70 accelerates atherosclerosis by downregulating the expression of ABCA1 and ABCG1 through the JNK/Elk-1 pathway. *Biochim Biophys Acta Mol Cell Biol Lipids*, 2018, **1863**(8): 806-822

MiR-216b通过靶向ABCG1促进破骨细胞形成并减少胆固醇流出*

杨五洲^{1)**} 黎恒^{1)**} 于小华^{2)**} 张洁¹⁾ 黄新云¹⁾
赵真旺¹⁾ 曹奇^{1)***} 唐朝克^{1)***}

¹⁾ 南华大学心血管疾病研究所, 动脉硬化化学湖南省重点实验室, 湖南省分子靶标新药研究协同创新中心, 南华大学附属第二医院, 衡阳 421001;

²⁾ 海南医学院第二附属医院临床医学研究所, 海口 460106)

摘要 目的 研究 miR-216b 在破骨细胞分化中的功能和靶基因, 探讨其对破骨细胞胆固醇外流的影响。方法 建立 RANKL 刺激诱导 RAW 264.7 破骨细胞前体细胞分化的细胞模型。进行抗酒石酸性磷酸酶 (TRAP) 染色测定以评估破骨细胞分化。通过生物信息学分析和双荧光素酶报告基因预测和分析 miR-216b 与其靶基因 ABCG1 3'非翻译区 (3'UTR) 的结合以及自由能。转染 miR-216b 模拟物或抑制剂以验证 miR-216b 在破骨细胞分化中的作用。液体闪烁计数用于测量来自 RAW264.7 巨噬细胞衍生的破骨细胞 [³H] 标记的胆固醇流出。通过高效液相色谱 (HPLC) 检测 RAW 264.7 巨噬细胞中的脂质积累。实时定量 PCR (RT-qPCR) 和蛋白质印迹分析用于评估破骨细胞中 ABCG1 的转录和转录后水平。结果 当细胞用 miR-216b 模拟物转染时, 破骨细胞的数量、破骨细胞的平均直径和融合指数显著增加, 如抗酒石酸性磷酸酶阳性染色和显微镜测定所揭示。MiR-216b 抑制剂显示出完全相反的结果, 这为我们的发现提供了额外的证据。生物信息学分析和双荧光素酶报告基因检测表明, miR-216b 靶向 ABCG1 的 3'UTR。进一步研究表明, miR-216b 抑制破骨细胞中 ABCG1 的 mRNA 和蛋白质水平。此外, 我们还发现 ABCG1 siRNA 对 ABCG1 的沉默增加了破骨细胞的数量、破骨细胞的平均直径和融合指数。MiR-216b 通过抑制 ABCG1 表达减少破骨细胞的胆固醇流出。结论 总的来说, 这些研究表明 miR-216b 下调 ABCG1 表达并抑制破骨细胞胆固醇流出, 从而扰乱胆固醇稳态并促进破骨细胞生成。

关键词 miR-216b, 破骨细胞, ABCG1, 胆固醇流出, 破骨细胞生成

中图分类号 Q2

DOI: 10.16476/j.pibb.2021.0014

* 国家自然科学基金(81770461)资助项目。

** 并列第一作者。

*** 通讯联系人。

唐朝克 Tel: 0734-8281853, E-mail: tangchaoke@qq.com

曹奇 Tel: 0734-8281853, E-mail: caoqi69@163.com

收稿日期: 2021-04-14, 接受日期: 2021-06-24